



UNIVERSITY OF TWENTE.

Faculty of Science & Technology

Robotic needle steering for prostate brachytherapy in a MR environment

Mart Johannes Wijntjes

M.Sc. Thesis

Juli 2022

Report Number: BE-875

Supervisors:

prof.dr. S. Misra (chairman)

dr. J.J. van den Dobbelsteen

dr. J. Sikorski

Surgical Robotics Group
Faculty of Faculty of Science & technology,
Biomedical Engineering
University of Twente
P.O. Box 217
7500 AE Enschede
The Netherlands

Summary

Brachytherapy is an internal radiation technology used to treat prostate tumors. Percutaneous needles are used to place catheters which place the radioactive beads. Accurate placement of these needles is currently a major limiting factor in transrectal ultrasound (TRUS) guided prostate brachytherapy. Real-time Magnetic Resonance Imaging (MRI) could offer an alternative form of visualisation with more accurate needle positioning. Robotic needle insertion could also greatly improve this targeting accuracy. Using flexible needles can improve targeting of positions that are usually hard to reach for rigid needles as well as correct for unexpected disturbances.

This study focuses on teleoperating a robotic system with a flexible needle attached to perform robotic MRI guided brachytherapy. The MIRIAM robotic system is developed by the Surgical Robotics Lab (SRL) at the University of Twente for MRI guided prostate biopsies and the flexible needle is developed by the 3ME group at the Delft University of Technology. The system is teleoperated using a daVinci Research Kit. Steering is performed by bending the proximal end of the needle which generates bending in the opposite direction of the distal end of the needle. Steering is performed in the horizontal plane. The main manipulator position defines the speed at which the needle base moves and the operator can switch between inserting the needle and moving the needle base continuously.

Three experiments are performed in the MRI scanner in the TechMed centre at the University of Twente and control is performed from the Horst building at the University of Twente. The system is teleoperated via an ethernet connection using the local network. Real-time MRI images are broadcasted to the operator using Microsoft Teams software. The experiments are performed in gelatin phantoms with 3d printed obstacles.

The experiments were performed successfully and 1 mm targets in positions unreachable by rigid needles were reached. This shows that MRI can be used to accurately guide teleoperated robotic prostate brachytherapy procedures.

Samenvatting

Brachytherapie is een interne bestralings methode die wordt toegepast om prostaat tumoren te behandelen. Percutane naalden worden gebruikt om een katether te plaatsen, hierdoor worden de radioactieve bestralingsbronnen geplaatst. Nauwkeurige plaatsing van deze naalden is op het moment een limiterende factor in transrectaal ultrasound (TRUS) begeleide prostaat brachytherapie. Real-time beeldvorming door magnetische resonantie (MRI) kan een alternatieve visualisatie methode bieden met nauwkeurigere beeldvorming van de naalden. Plaatsing van de naalden met behulp van robotica kan menselijke fouten verminderen en op die manier zorgen voor verbeterde resultaten. Het gebruik van flexibele naalden kan er voor zorgen dat doelwitten achter obstakels ook bereikt kunnen worden.

Deze studie focust zich op de teleoperatie van een robotisch systeem met een flexibele naald er aan bevestigd. Dit systeem zal in een MRI omgeving het aanprikken van doelwitten voor brachytherapie uitvoeren. De MIRIAM robot is ontwikkeld door het Surgical Robotics Lab (SRL) aan de Universiteit Twente voor MRI begeleide prostaat biopsies en de flexibele naald is ontwikkeld door de 3ME vakgroep aan de technische Universiteit van Delft. Het systeem wordt doormiddel van teleoperatie aangestuurd door een daVinci Research Kit (dVRK). Het sturen van de naald wordt uitgevoerd door de achterkant van de naald te buigen, dit levert aan de punt buiging in de tegenovergestelde richting op. Voor deze studie zal alleen gestuurd worden in het horizontale vlak. De positie van de dVRK manipulator bepaald de snelheid waarmee de basis van de naald wordt verplaatst, de clinicus kan continu wisselen tussen verplaatsing van de naald en het invoeren van de naald.

Drie experimenten worden uitgevoerd in de MRI ruimte in het TechMed center aan de Universiteit Twente. Het systeem wordt bij deze experimenten aangestuurd van het Horst gebouw aan de Universiteit Twente. De verbinding tussen de twee systemen gaat via het lokale ethernet netwerk. De MRI beelden worden continu gestreamd doormiddel van Microsoft Teams software. De experimenten worden uitgevoerd in gelatine fantomen met 3d geprinte obstakels.

De uitgevoerde experimenten zijn succesvol uitgevoerd en doelwitten met een diameter van 1 mm op posities die slecht te bereiken zijn voor stijve naalden zijn succesvol bereikt. Dit laat zien dat MRI een goed alternatief kan zijn voor het begeleiden van robotische prostaat brachytherapie.

Preface

This thesis is written as part of my Master's assignment for my Biomedical Engineering program at the University of Twente. This project would not have been possible without the help of many people but there are several people I would like to thank in particular. First of I would like to thank Sarthak Misra for giving me the opportunity to do this assignment at the Surgical Robotics Lab. I've thoroughly enjoyed working in this great environment. I would also like to thank John van den Dobbelen for being part of my Master's assignment committee, the few meetings we've had were very valuable to me and have helped me shape this project to what it has eventually become. Next I would like to thank Jakub Sikorski for guiding me through this Master's assignment. Your availability and helpful advice has given me great insights and feedback on my work. Without your help this project would not have been possible. Next I would like to thank Martijn de Vries for helping me with many aspects of the project and helping me preparing the phantom for the experiments. I would also like to thank Nick van de Berg and Remco Liefers for helping me shape and guide the experiments performed for this project. Finally I would like to thank everyone that helped me during my time at the Surgical Robotics Lab, I've really enjoyed working at this group and felt welcomed from my first day at the lab.

Mart Wijntjes
Enschede, June 2022

Contents

Page No.

1	Introduction	10
2	Robotic needle steering for prostate brachytherapy in a MR environment	14
2.1	Introduction	15
2.2	Design	15
2.3	Control	16
2.3	Experimental Protocol	19
2.4	Results	20
2.5	Discussion	21
2.5	Conclusions	22
3	Discussions & Conclusions	25
	Appendices	26
A	Production of a gelatin prostate phantom	28
B	Remote system latency test	30

Chapter 1

Introduction

Cancer is the third leading cause of death worldwide [1]. Malignant tumors in the prostate are the most frequent occurring type of cancer and second highest cause of cancer related deaths among man. For women malignant tumors in the breast and uterine are very frequent occurring types of cancer [2]. A variety of treatment options are available for treatment of these tumors with the standard approaches being radiotherapy (RT) and surgical removal of the prostate. RT is a minimally-invasive alternative to surgical removal with proven ability to provide good oncological outcomes [3]. For high rates of success tumor treatment sufficiently high RT dose are required [4]. There are two main modalities for applying RT, external-beam radiotherapy generated by a linear accelerator or brachytherapy (BT) generated by implantation of radioactive sources directly into the malignant tissue [5]. Unlike external-beam RT, brachytherapy radiates the tumor from within. The radioactive sources are placed using catheters. Percutaneous medical needles are used to place the catheter at the target location inside the tumor. There are two forms of BT, permanent and temporary implantation. In BT different rates at which dose is delivered can be applied. This is known as the dose rate and is different for permanent and temporary implantation. The International Commission on Radiation Units Measurements defines the following dose rates[6]:

- Low Dose Rate (LDR), 40 - 200 cGy per hour (cGy/h)
- Medium Dose Rate (MDR), 200 - 1200 cGy/h
- High Dose Rate (HDR), 1200+ cGy/h

Permanent BT for prostate uses radioactive sources with LDR. Temporary BT on the contrary uses HDR for high radiation over a small period of time [7].

The advantage of BT over external RT is that the procedure is minimally invasive and can more accurately radiate the target tissue without also radiating other tissue. The procedure remains minimally invasive because percutaneous needles are used. The advantage of percutaneous procedures over traditional surgical procedures are that only a very small hole through the skin is required. This results in shorter recovery times and decreased chance of secondary wound infection/stomatitis [8].

Accuracy of the needle placement is an important determining factor in the rate of success of the procedure. For many of these procedures mistargeting and missing the place of interest can lead to undertreatment of the tumor and it will require additional needle placement. This will ultimately result in excessive tissue damage and decreased therapy effectiveness. Accurate needle placement still poses a major challenge [9]. Traditionally rigid needles are used for percutaneous procedures, these needles are restricted to a straight needle insertion path. Due to the nature of these needles and the tissue interactions targeting errors occur for deep insertions [10]. Current needles used for BT are rigid needles made of 1.47 or 1.27 mm steel, despite this they still deflect. This is mainly due to the assymetric forces that arise from the bevel tip needle geometry [11]. In these procedures the insertion already starts deviated resulting from contact between the needle and the skin [12]. These deviations are difficult to correct without a steerable needle. There are several other factors that can influence the accuracy of the needle placement like physician's error, tissue movement, deformation and imaging limitations.

With the use of rigid needles physician have limited tools at their disposal for correcting for these errors. To reduce placement errors physicians can retract and repeatedly reinsert the needle with slight adjustments [9]. This can cause longer procedure times and excess tissue damage. There is therefore a desire for improved needle insertion accuracy. Steerable needles could prove to be useful in increasing targeting accuracy [13].

There are two types of needle steering: passive and active needle steering. It is important that the needle is flexible because in both cases the needle bends during insertion. Passive needle steering is induced by the needle-tissue interaction. Asymmetric tips can induce rotation through the tissue as a result of the insertion force. Active needle steering is steering in which the tip or the shape of the

needle can be actively changed regardless of the needle-tissue interaction. Active steering can be achieved by using cable-driven instruments or actuated needle tips [14]. Flexible needles also offer the possibility to reach subsurface targets that would otherwise be inaccessible for rigid needles due to obstacles like sensitive tissues blocking the path [15]. Steering flexible needles manually without feedback can be difficult due to the limitations in human control. [16]

Current BT procedures are ultrasound guided. A transrectal ultrasound (TRUS) probe is used to assist the recreation of the pre-operative planning and assure that the needles are placed in the predefined location [5]. With TRUS guided brachytherapy great care should be taken in avoiding trauma to the bladder, urethra and rectum caused by needle insertion. TRUS is cheap and widely available for interventions. However, it is impossible to see the tumor or any internal prostate structure in the images. Post-operative computer tomography (CT) imaging can be used to confirm implant placement. Magnetic resonance imaging (MRI) could present a solution to these issues, with the increased capabilities of MRI real-time imaging is possible [17]. MRI has a higher signal-to-noise ratio and high imaging accuracy compared to ultrasound imaging. Unlike TRUS MRI can visualise internal prostate structure. This could result in better tumor targeting in BT [18]. MR environments can add complexity to the procedure, since all tools used have to be non-magnetic and the workspace is limited.

In this thesis we developed a MRI-guided needle insertion system for BT. The system integrates an active needle, a MRI-compatible needle insertion robot, and a teleoperating platform. This system can perform robotic BT procedures using flexible needles and solves many of the current limitations of BT procedures. The system can be teleoperated limiting the structural impact the system on the MR room, ensuring that the system is applicable to nearly any MR room.

The next chapter of this thesis will be the results of this work in the form of a paper.

References

- [1] C. D. Mathers, T. Boerma, and D. Ma Fat, “Global and regional causes of death,” *British Medical Bulletin*, vol. 92, no. 1, pp. 7–32, Sep. 2009, ISSN: 0007-1420. DOI: 10.1093/bmb/ldp028. eprint: <https://academic.oup.com/bmb/article-pdf/92/1/7/948940/ldp028.pdf>. [Online]. Available: <https://doi.org/10.1093/bmb/ldp028>.
- [2] R. L. Siegel, K. D. Miller, and A. Jemal, “Cancer statistics, 2018,” *CA: A Cancer Journal for Clinicians*, vol. 68, pp. 7–30, 1 Jan. 2018, ISSN: 00079235. DOI: 10.3322/caac.21442.
- [3] R. M. Galalae, A. Martinez, N. Nuernberg, *et al.*, “Hypofractionated conformal hdr brachytherapy in hormone naïve men with localized prostate cancer,” *Strahlentherapie und Onkologie*, vol. 182, pp. 135–141, 3 Mar. 2006, ISSN: 0179-7158. DOI: 10.1007/s00066-006-1448-5.
- [4] T. M. Pisansky, “External-beam radiotherapy for localized prostate cancer,” *New England Journal of Medicine*, vol. 355, pp. 1583–1591, 15 Oct. 2006, ISSN: 0028-4793. DOI: 10.1056/NEJMct055263.
- [5] G. Koukourakis, N. Kelekis, V. Armonis, and V. Kouloulis, “Brachytherapy for prostate cancer: A systematic review,” *Advances in Urology*, vol. 2009, pp. 1–11, 2009, ISSN: 1687-6369. DOI: 10.1155/2009/327945.
- [6] “Dose and volume specification for reporting interstitial therapy,” Office of Scientific and Technical Information, Dec. 1997. DOI: 10.2172/672130.
- [7] B. W. Fischer-Valuck, H. A. Gay, S. Patel, B. C. Baumann, and J. M. Michalski, “A brief review of low-dose rate (ldr) and high-dose rate (hdr) brachytherapy boost for high-risk prostate,” *Frontiers in Oncology*, vol. 9, Dec. 2019, ISSN: 2234-943X. DOI: 10.3389/fonc.2019.01378.
- [8] P. Brass, M. Hellmich, A. Ladra, J. Ladra, and A. Wrzosek, “Percutaneous techniques versus surgical techniques for tracheostomy,” *Cochrane Database of Systematic Reviews*, Jul. 2016, ISSN: 14651858. DOI: 10.1002/14651858.CD008045.pub2.
- [9] H. Sadjadi, K. Hashtrudi-Zaad, and G. Fichtinger, “Needle deflection estimation: Prostate brachytherapy phantom experiments,” *International Journal of Computer Assisted Radiology and Surgery*, vol. 9, pp. 921–929, 6 Nov. 2014, ISSN: 1861-6410. DOI: 10.1007/s11548-014-0985-0.
- [10] Y. R. van Veen, A. Jahya, and S. Misra, “Macroscopic and microscopic observations of needle insertion into gels,” *Proceedings of the Institution of Mechanical Engineers, Part H: Journal of Engineering in Medicine*, vol. 226, pp. 441–449, 6 Jun. 2012, ISSN: 0954-4119. DOI: 10.1177/0954411912443207.
- [11] S. Misra, K. B. Reed, A. S. Douglas, K. T. Ramesh, and A. M. Okamura, “Needle-tissue interaction forces for bevel-tip steerable needles,” in *2008 2nd IEEE RAS EMBS International Conference on Biomedical Robotics and Biomechatronics*, 2008, pp. 224–231. DOI: 10.1109/BIOROB.2008.4762872.
- [12] P. Moreira, N. Patel, M. Wartenberg, *et al.*, “Evaluation of robot-assisted mri-guided prostate biopsy: Needle path analysis during clinical trials,” *Physics in Medicine Biology*, vol. 63, 20NT02, 20 Oct. 2018, ISSN: 1361-6560. DOI: 10.1088/1361-6560/aae214.
- [13] P. Moreira, G. van de Steeg, F. van der Heijden, J. J. Futterer, and S. Misra, “A preliminary evaluation of a flexible needle steering algorithm using magnetic resonance images as feedback,” *IEEE*, Aug. 2014, pp. 314–319, ISBN: 978-1-4799-3128-6. DOI: 10.1109/BIOROB.2014.6913795.
- [14] N. Berg, “Needle steering mechanics and design cases,” Ph.D. dissertation, Oct. 2016. DOI: 10.4233/uuid:bdb314b6-9346-4054-9962-d7038999b3ad.
- [15] S. Misra, K. Reed, B. Schafer, K. Ramesh, and A. Okamura, “Mechanics of flexible needles robotically steered through soft tissue,” *The International Journal of Robotics Research*, vol. 29, pp. 1640–1660, 13 Nov. 2010, ISSN: 0278-3649. DOI: 10.1177/0278364910369714.
- [16] M. Abayazid, C. Pacchierotti, P. Moreira, R. Alterovitz, D. Prattichizzo, and S. Misra, “Experimental evaluation of co-manipulated ultrasound-guided flexible needle steering,” *The International Journal of Medical Robotics and Computer Assisted Surgery*, vol. 12, pp. 219–230, 2 Jun. 2016, ISSN: 14785951. DOI: 10.1002/rcs.1680.

- [17] K. S. Nayak, Y. Lim, A. E. Campbell-Washburn, and J. Steeden, “Real-time magnetic resonance imaging,” *Journal of Magnetic Resonance Imaging*, vol. 55, pp. 81–99, 1 Jan. 2022, ISSN: 1053-1807. DOI: 10.1002/jmri.27411.
- [18] A. Peltier, F. Aoun, M. Lemort, F. Kwizera, M. Paesmans, and R. V. Velthoven, “Mri-targeted biopsies versus systematic transrectal ultrasound guided biopsies for the diagnosis of localized prostate cancer in biopsy naïve men,” *BioMed Research International*, vol. 2015, pp. 1–6, 2015, ISSN: 2314-6133. DOI: 10.1155/2015/571708.

Chapter 2

Robotic needle steering for brachytherapy in a MR environment

This chapter a paper is presented on robotic needle steering for brachytherapy in a MR environment. This paper was written as part of this master thesis.

Robotic teleoperated needle steering for brachytherapy in a MR environment

Mart Wijntjes¹, Martijn de Vries¹, Jakub Sikorski, Pedro Moreira, Nick van de Berg,
John J. van den Dobbelsteen, Sarthak Misra

Abstract—Brachytherapy is internal radiotherapy performed by placing radioactive sources under ultrasound guidance. This method is currently limited in accurate needle placement and visualisation capabilities. As a solution to these limitations this study presents a system that performs magnetic resonance imaging (MRI) guided teleoperated needle steering using an active needle system. A daVinci Research Kit teleoperates a magnetic resonance (MR) compatible robot with a flexible needle attached while real-time MRI images are feedbacked to the operator. First, teleoperated needle steering in a cervical phantom are performed. After this circumventing organs at risk (OARs) experiments in a prostate phantom are performed. Targets are placed behind the urethra and pubic arch in positions hard to reach for traditional rigid needles. During these experiments 1mm targets at depths up to 100mm are reached with an average error of 1.2mm (n=10).

Index Terms—MRI, brachytherapy, needle steering, teleoperation, daVinci Research Kit

I. INTRODUCTION

Cancer is among the leading causes of death worldwide [1]. Malignant tumors in the prostate are the most frequent occurring type of cancer and second highest cause of cancer related deaths among men [1]. For women malignant tumors in the breast and uterus are very frequent occurring types of cancer [2]. A variety of treatment options are available for treatment of these tumors with the standard approach being surgical removal of the tumor. Surgical removal is an invasive procedure that can result in long recovery and possible infection. Radiotherapy is a non-invasive alternative to surgical removal with proven ability to provide good oncological outcomes [3].

Brachytherapy is a form of internal radiotherapy where radioactive sources are placed inside the malignant tissue. Radioactive sources are placed in the target tissue using rigid percutaneous needles and ultrasound visualisation for guidance. [4]–[7]. This technique has the advantage that high radiation dose is delivered to the target tissue while surrounding healthy tissue is spared. However, this method presents limited visual feedback as internal structures are indistinguishable. [8]. Accuracy of needle placement is an important determining factor in dose delivery [9]. For many of these procedures mistargeting and missing the place of interest can lead to undertreatment of the tumor, this still poses a major challenge [10]. Traditionally, rigid needles are used for percutaneous procedures and only straight needle insertions are considered. However, due to the nature of these

needles and the tissue interactions targeting errors are not uncommon and are closely related to insertion depth [11], [12]. Flexible needles have the potential to be more precise than rigid needles if they are properly controlled and can avoid sensitive structures [13]–[15].

MR compatible robotics have shown to be capable of performing accurate MRI guided needle insertion while inducing minimal signal-to-noise. [12], [16], [17].

This work is intended to develop a system able to steer a flexible needle using real-time MRI visual feedback. A MRI-guided needle insertion system that integrates an active steerable needle and a MR compatible robot is presented. The system is teleoperated online using daVinci surgical systems. The system presents a solution to current radioactive source placement for BT limitations in the form of teleoperated MRI-guided brachytherapy as shown in figure 1. The system is designed to function in every MR scanner without structural changes required to the MR room. This creates a versatile system that expands current functionality of the MR room.

II. DESIGN

The teleoperated needle steering for brachytherapy in a MR environment system was developed by integrating three existing systems. This section will explain how the integration of the three subsystems was designed. First the components will be explained and how physical connection between the needle and the robot is realised.

A. Components

In our approach, the radioactive source placement is performed using an axial stiff steerable needle with compliant active tip control [18]. The needle consists of an outer catheter of polyamide and a steerable super elastic nitinol inner needle. The inner needle can be retracted from the outer catheter to leave a working channel for radioactive source placement. The inner needle is a single-piece rod cut in four segments along the longitudinal axes of the rod while keeping the ends of the needle connected as one piece. The middle of the needle is supported by rollers as shown in figure 2. Lateral steering of the proximal end of the needle will result in extension of one of the segments and a compression of the opposite segment. The resulting pulling and pushing forces are transferred through the segments and result in lateral movement of the distal end in the opposite direction, this principle is visualised in figure 2.

1. Mart Wijntjes and Martijn de Vries contributed equally to this work

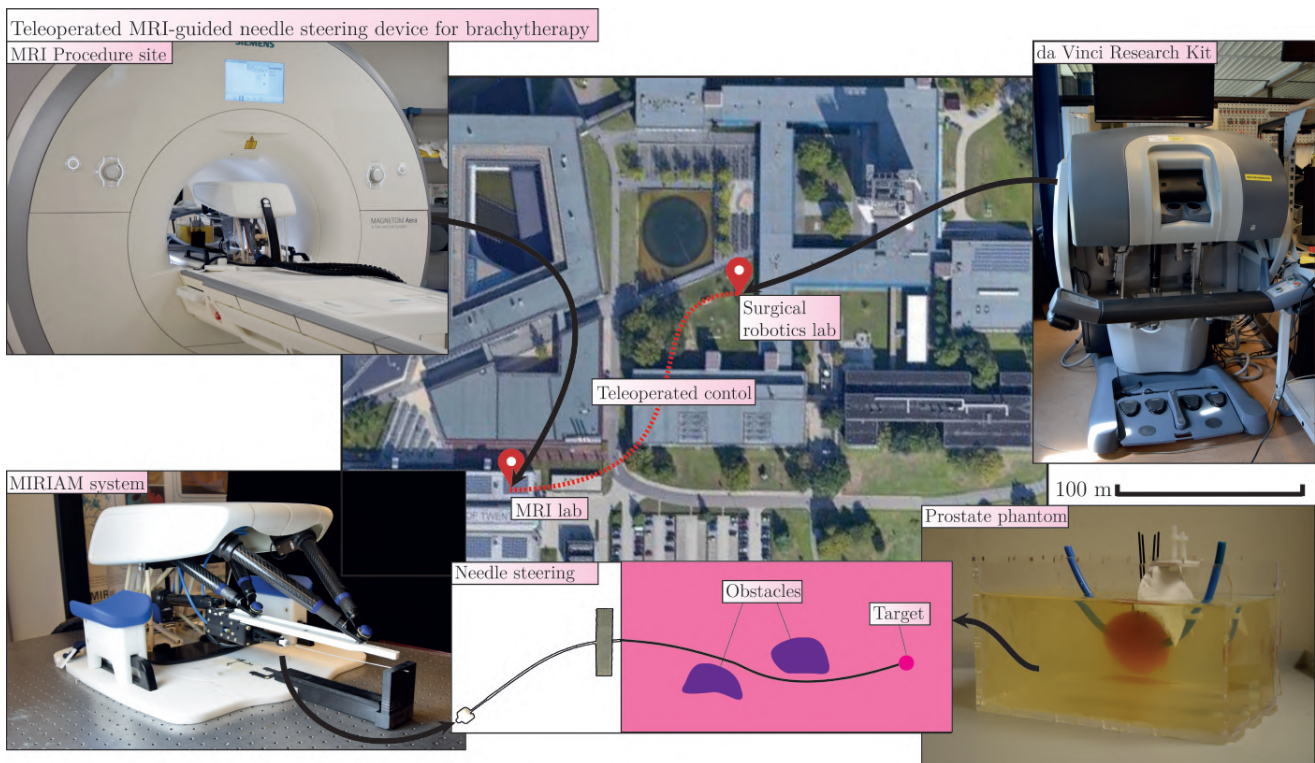


Fig. 1. A teleoperated magnetic resonance imaging (MRI) guided needle placement system is visualised. The minimally invasive robotics in a magnetic resonance environment system is placed in MRI bore and performs needle steering towards a assigned target. In this case these targets are placed inside a prostate phantom. The entire system is teleoperated using a dVRK that controls the system using an ethernet connection using the local network, this controller is placed in the Surgical Robotics Lab. MRI images are feedbacked to the operator at the controller end of the system.

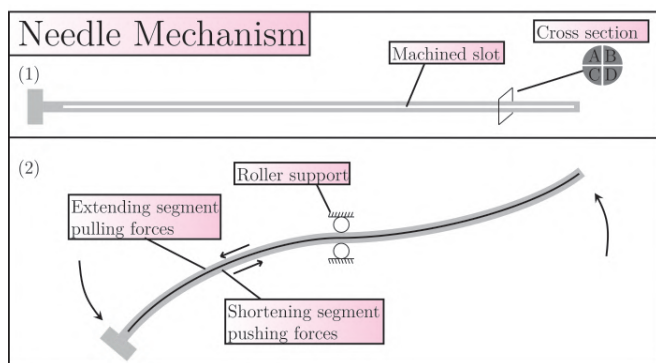


Fig. 2. (1). Side view of needle in neutral position with machined slot in the middle, and a front view of the same slot. (2). Steering of the needle as a result of the internal forces in the needle caused by applying a force at the proximal end of the needle. The internal forces cause an opposite movement of the distal end of the needle.

The targeting of the needle within the MRI bore is performed by Minimally invasive robotics in a MR environment (MIRIAM), which is a MR compatible 9 DoF robotic system utilizing piezo-electric motors for needle positioning and insertion. The robot was made from non magnetic materials to ensure MRI safety. The base structure is made from ceramics rods, the needle guide is positioned using five extendable carbon rods. The rods, insertion and rotation of the needle are actuated using HR2 and HR8 piezo-electric motors by

Nanomotion (Yoqneam, Israel) [19]. The needle firing system is actuated using high pressure air. The low level controller and motor drivers are located in a control tower placed outside of the MRI room and is tethered using 10m long cables.

In order to keep the structural changes to the MRI room minimal the MIRIAM platform is operated using a da Vinci Research Kit (dVRK, Intuitive Surgical, Sunnyvale, CA, USA) [20]. The dVRK system is a research version of the Da Vinci Surgical that is a widely used clinical robot. dVRK allows for low-level access to DaVinci MTM inputs/outputs. A stereo viewer allows the operator to receive visual feedback. The kit is shown in figure 1.

B. MIRIAM hardware adaptations

The MIRIAM platform was adapted to facilitate the attachment of the new needle system. The pneumatic actuation of the biopsy needle was no longer required and disabled for this system. The original biopsy needle is replaced with the axial stiff steerable needle. This needle is attached using a hinge joint supported using a needle guide template as shown in figure 3.

III. CONTROL

The system presented in this article is teleoperated from a location separate from the MR room. The MIRIAM robot is teleoperated using the the DaVinci manipulators. There are three logical control laws that could be chosen for the

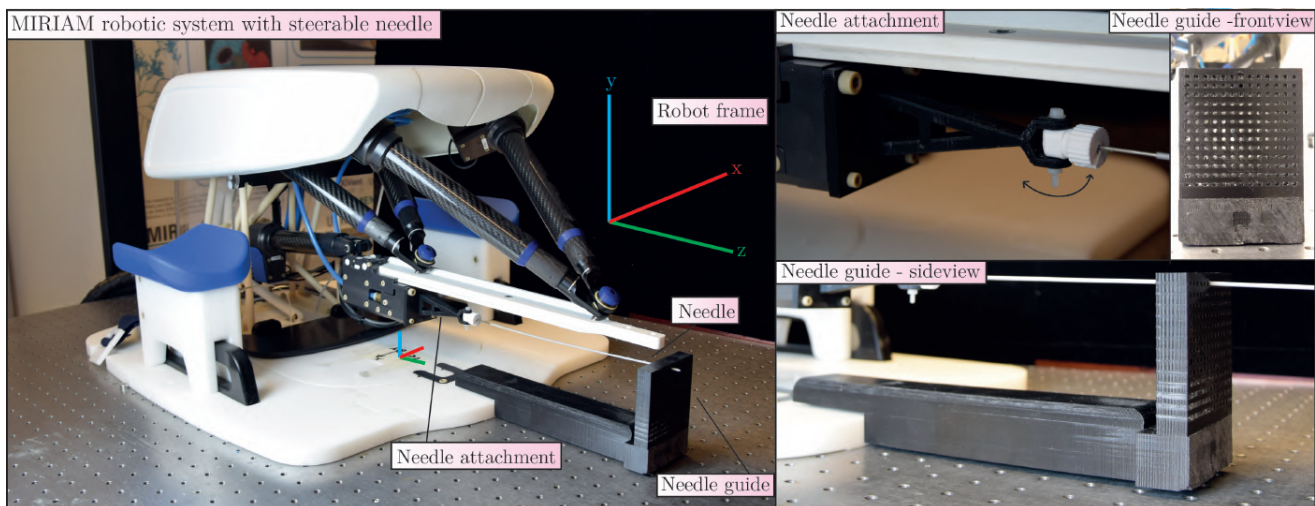


Fig. 3. The minimally invasive robotics in a magnetic resonance environment system is a robotic system used for automated needle insertions in magnetic resonance environments. For this work the needle is attached using a hinge joint. The needle is supported using a needle guide.

teleoperation: position control, velocity control or acceleration control. In each case the input is the position of manipulator and the control law determines the output that is sent to the MIRIAM robot based on this input.

For the selection of a control law for our system there are several important factors to take into consideration. The first consideration is the intuitivity of the system, the end goal is for a physician to control the MIRIAM robot for medical procedure, therefore a large learning curve and unpredictable behaviour are undesired. Another consideration is that it is important that the system can be held in a constant position when inserting the needle. The last consideration is that the system can be controlled accurately for precise needle insertions.

To control the MIRIAM robot velocity control was chosen. In Velocity control the controller is always at the same position when released, this is very intuitive as the operator is looking at a screen and can easily find the manipulator at a known location.

As mentioned in section II-B needle steering is only performed in the XZ-plane, for this reason only the movement in the X-direction is teleoperated. The eventual teleoperation was performed using the following control law:

$$v = k \cdot (x - x_0) \quad (1)$$

where v is needle base velocity, k is a scaling constant x is the current manipulator position and x_0 is the starting manipulator position.

A. Communication setup

There is continuous exchange of information between the MIRIAM system and dVRK system. Operating this continuous exchange of information through the local area network (LAN) provides plug and play possibilities for the system. A user datagram protocol (UDP) is developed for sending and receiving information between several subsystems. On the dVRK

end robotic operating software (ROS) version Noetic Ninjemys is used. On the MIRIAM end MATLAB 2016b is used. The protocol handling the communication between MIRIAM and the dVRK is shown in algorithm 1.

Algorithm 1 Communication algorithm MIRIAM

User initiates communication
New dVRK ▷ dVRK Object
New MIRIAM ▷ MIRIAM Object
New UDP ▷ UDP Object

function UDP_SEND(sender, variables, receiver)
 Sends *variables* from *sender* to *receiver* on object *UDP*
end function

function SCAN(receiver, Object)
 Scans *Object* for new messages send to *receiver*
end function

repeat
 $dVRK_pos = dVRK.manipulator_position$
 $UDP_send(dVRK, dVRK_pos, MIRIAM)$
 $MIRIAM_input = Scan(MIRIAM, UDP)$
 $MIRIAM.move(MIRIAM_input)$
 $MIRIAM_pos = MIRIAM.current_position$
 $UDP_send(MIRIAM, MIRIAM_pos, dVRK)$

$dVRK_in = Scan(dVRK, UDP)$
 $dVRK.visual(dVRK_in)$

until user terminates

B. MIRIAM software adaptation

MIRIAM is originally designed for a single movement of the needle guide to a target position followed by needle

insertion. In the current application it is desired that the needle guide movement and insertion states can be switched between continuously. The MIRIAM software is reprogrammed to switch between movement and insertion state triggered by the position of the gripper. During operation there are continuous safety checks going on. One of these checks is to see if the rods have reached the desired length to reach a set-point. A new set-point would only be accepted if this check is completed. Since the inputs into the system for teleoperation are continuously processed the set-point is updated frequently. When removing these safety checks all set-points are processed which makes MIRIAM movement extremely slow. This is solved by only sending a set-point for every N rotations of communication between MIRIAM and the dVRK computers. This will decrease the amount of set-points that are processed and will in turn increase the speed. Using this method a balance between speed and accuracy can be found with the current software. N was experimentally tuned to be $N = 50$.

C. MIRIAM movement

The input from the dVRK has to be converted to a movement of MIRIAM. In the movement state the position from the manipulator is continuously received and converted to the deflection of the manipulator from the zero position as following $\Delta x = x - x_0$ and this Δx is multiplied by a scaling constant k . This constant was experimentally determined to be $k_{move} = 0.005$. As we defined in function 1 the output is a velocity. The input for MIRIAM is a position set-point. Since the velocity is a change in position we can say the following:

$$v = \frac{\Delta x}{\Delta t} \quad (2)$$

where v is the velocity, x is the position and t is time. From now on we will treat the Δx of the set-point as Δpos . As we want the pos_{new} as the input to our system and the MIRIAM is a discrete system we can say that function 3 can be applied for every time step ($dt=0.01$).

$$pos_{new} = pos_{old} + k \cdot \Delta x \quad (3)$$

where k is a scaling factor and Δx is the change in manipulator position in the x direction with regards to the begin position of the manipulator. Function 3 is used to change the set-point for MIRIAM based on the input of the dVRK manipulator. After this the X , Y and Z set-point is sent to MIRIAM Simulink Real-Time system.

In the insertion state the same principle is applied to the the following function for the set-point with the scaling factor $k_{ins} = 0.005$:

$$pos_{new} = pos_{old} + k \cdot \Delta z \quad (4)$$

where k is again a scaling factor and Δz is the change in manipulator position in the z direction with regards to the begin position of the manipulator. This method directly translates sideways motion of the manipulator to a sideways motion of the needle base. Direct sideways movement of the needle base will cause needle retraction or insertion. Instead

of perpendicular movement to the needle fixation point the base of the needle should make an arc like motion as shown in figure 4. If the needle base is moved in a straight line like shown in figure 4.b the length ($L2$) will be greater than ($L1$) and thus retracting the needle. When moving the needle base in an arc as shown in figure 4.c the length ($L3$) will remain the same as ($L1$) over the entire motion and thus not inserting or retracting the needle.

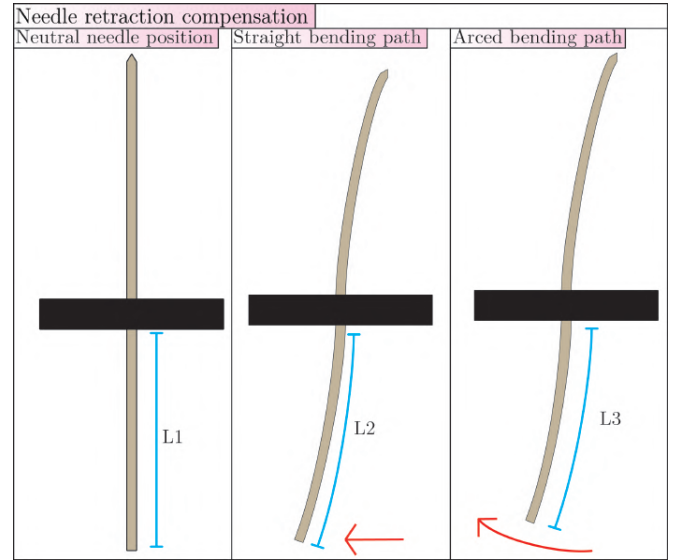


Fig. 4. Needle bending should be performed in an arc motion around the template insertion point to prevent unwanted retraction of insertion as a result of needle bending. Figure b shows needle bending with a straight path, the red arrow demonstrates the movement of the needle base without compensation, this way the length $L2$ will be greater than $L1$ and thus retracting the needle. Figure c shows bending with an arc motion, the red arrow demonstrates the movement of the needle base with compensation, this way the length $L3$ will be equal to $L1$ and thus not retracting the needle.

The arc the needle makes depends on how far the needle is inserted into to template. At intervals of 20mm of insertion the needle base is moved perpendicularly to the fixation point at movement intervals of 10mm. At every point the amount of needle retraction is measured. The maximum amount of needle retraction is shown in table I. These values were measured at a deflection of 100mm from the center-line. For each insertion depth ten data points were acquired, using the *fit* function in MATLAB 2016b a second order polynomial was fit to the data points. A visualisation of this fit at 0mm, 60mm and 140mm is shown in figure 5.

The amount of needle retraction is added to the movement of the needle base in the Z direction based on the insertion depth and the actual position of the needle base. When inserting the needle at a deflection from the center-line the calculated amount of needle compensation changes. To prevent undesired needle insertion or retraction when changing between insertion depths a correction factor is applied when changing between insertion depths. This correction factor is the compensation at the previous insertion depth minus the compensation calculated for the new insertion. This difference is added to the actual needle compensation to prevent changes in compensation when changing between different insertion

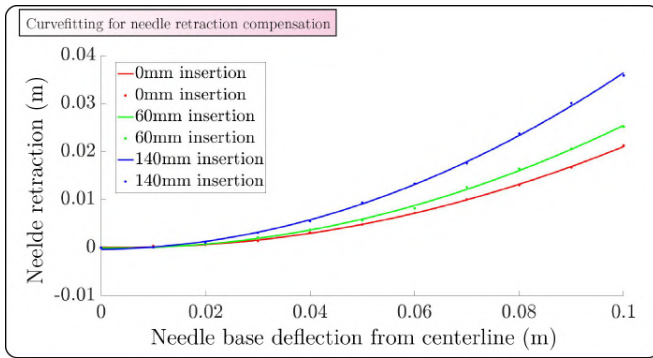


Fig. 5. Needle retraction at 0mm, 60mm and 140mm insertion. Data points at step size of 10mm away from center-line

TABLE I

MAXIMUM NEEDLE RETRACTION AT EIGHT INSERTION DEPTHS, ALL MEASURES FOR MAXIMUM NEEDLE RETRACTION WERE FOUND AT 100MM DEFLECTION FROM THE CENTER-LINE

Insertion depth (mm)	Maximum needle retraction (mm)
0	21.24
20	21.66
40	22.81
60	25.2
80	27.6
100	30.7
120	31.3
140	35.8

depths.

D. Visualization

The surgical procedures are performed in a MR environment while the physician performs procedure outside of the MR room. Continuous visual feedback is provided to the physician. The visualization is updated with the current and set-point positions through the communications protocol as mentioned in III-A. Using this information the current position of the MIRIAM robot and the set-point position of MIRIAM are visualized. Since MIRIAM movement is relatively slow the visualization method can give the physician a live update on the movements the MIRIAM robot will make as a result of the inputs given at the manipulator as well as an indication of when MIRIAM is finished moving to the set-point.

The MRI system used for the experiments is a Siemens Magnetom AERA 1.5T. Images are taken with the following parameters: T1W-TF2D scan with FOV = 191x272 mm; flip angle = 70 TR/TE = 250.85/1.24 ms; voxel size= 1.31 x 1.31 mm; slice thickness = 8 mm; number of slices = 1.

MRI systems have closed source software, therefore extracting specific imaging sources from the system can be complex. The MRI system used for this project has a video capture card attached to it that allows an HDMI signal to be converted to an USB video input. This HDMI output is the same signal as the control computer. For visual feedback this video signal is send to the physician using Microsoft Teams software. Further integration of this video feedback lies outside of the scope of this research.

IV. EXPERIMENTAL PROTOCOL

In order to validate the functioning of the system and prove clinical application several experiments are performed. The first experiments are performed outside of the MRI bore to test the steering and needle insertion compensation. After this experiments are performed to test the functionality of the system in a MRI environment. For all these experiments different phantoms are produced.

A. Steering and needle compensation experiments

The first experiment is performed to test the communication, teleoperation and needle steering. This experiment was performed in many iterations through the engineering process. The final version of this experiment confirms the operation of all systems. For the final version of this experiment the needle is steered into a gelatin phantom.

As mentioned in section II-B a needle compensation algorithm was designed to make sure MIRIAM moved around the fixation point of the needle with an arc like motion as shown in figure 4. In this experiment the performance of this compensation algorithm is tested by comparing the maximum needle retraction at a lateral deflection of 10 cm with and without the compensation algorithm active. This retraction is be tested at three insertion depths 0mm, 50mm, 100mm. This gives an indication of how much the algorithm reduces the undesired needle insertion/retraction.

B. MRI experiments

For this project three experiments were performed in the MRI lab in the Technical Medical Centre at the University of Twente. The MIRIAM robot was placed in the MRI bore while the dVRK was placed in the Surgical Robotics Lab at the University of Twente. These two systems were placed in different university buildings. The first experiment was used as a proof of concept to test if all the systems were functional. The second and third experiment were performed for more clinical relevant results.

Experiment 1: Needle steering in cervix phantom: The first experiment is performed in a gelatin cervix phantom, the gelatin is made using 100g of Dr. Oetker gelatin powder per liter of water. Inside the phantom two solid 3d printed obstacles are placed that should be avoided during needle insertion. Three square pieces of chicken with dimensions of 5x5mm are placed in the gelatin to act as a target. The pieces of chicken are placed at a depth of approximately 130mm. Systems to validate are the following: the functioning of the MIRIAM robot in a MR environment, the visual feedback of real-time MRI and the functioning of the communication protocol and to check the functioning of the online communication protocol between different buildings. The second goal of this experiment is to test the steering and targeting abilities of the system.

Experiment 2: Circumventing organs at risk (OARs) in prostate phantom: The second experiment is performed using a anatomically correct prostate phantom. The phantom was based on patient data and made to scale involving the following components:

- Prostate - (3% SiO_2 + 6.8% Polyvinyl alcohol (PVA) + 72.2% Dimethyl sulfoxide (DMSO) +18% demineralised H_2O)
- Adipose tissue - (6% PVA + 75% DMSO + 19% demineralised H_2O)
- Pubic arch - Acrylonitrile butadiene styrene
- Urethra - flexible rubber rod
- Target rods - carbon 1mm diameter

The prostate is made using a mould based on patient data as shown in figure 6 The goal of this experiment is to target positions behind the urethra that can't be reached by traditional rigid needles in a clinically relevant environment. A visualization of the phantom is shown in figure 7.

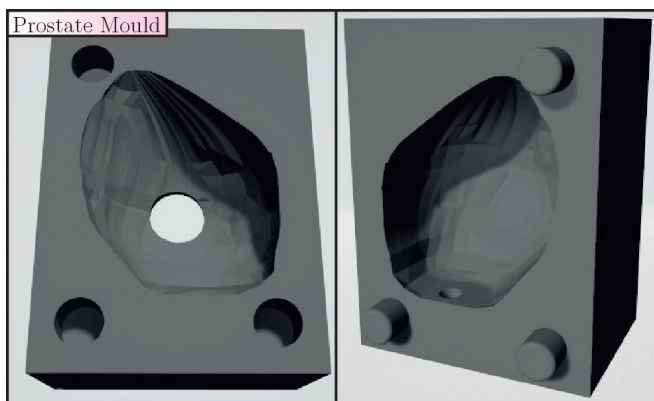


Fig. 6. A prostate mould based on patient data from magnetic resonance images used to create a gelatin prostate.

This experiment is performed a second time in a phantom with a similar design. For this phantom the prostate and adipose tissue were produced using gelatin using 100g of Dr. Oetker gelatin powder per liter of water.

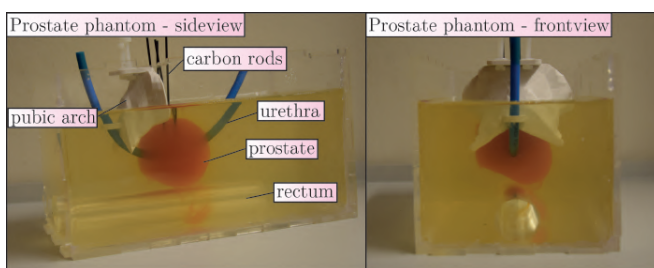


Fig. 7. A prostate phantom based on patient data made out of Dr. Oetker gelatin. Showing a sideview with the prostate, pubic arch, urethra, rectum and carbon target rods labeled.

As real-time MRI is used the resolution of the images is relatively low and artifacts around needle tips are common in MRI it can be hard to identify the exact position of the needle tip. In order to determine the distance between the needle tip and the target for each insertion the needle and target are segmented in post-processing. A second order polynomial is fit to the needle and extended to the approximate position of the tip. The distance from this point and the target is determined.

V. RESULTS

The maximum measured lateral displacement of the needle tip in a gelatin sample is 35mm at an insertion depth of 120mm. The maximum movement speed of the base of the needle is approximately $1 \cdot 10^{-3}m/s$. The maximum insertion speed of the base of the needle is approximately $2 \cdot 10^{-2}m/s$. The latency between the two system averages at 8.5ms (min 0.43 ms - max 51.7 ms) for the needle control. A MRI image is send every 2 seconds.

A. Experiment result

The communication, teleoperation and needle steering tests were performed successfully and an image of a needle deflection test in gelatin is shown in figure 8.

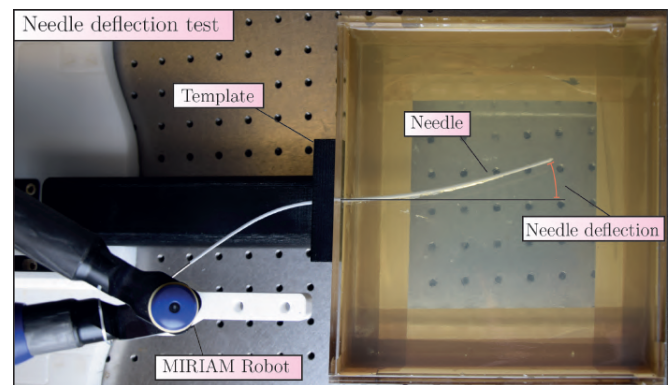


Fig. 8. Needle deflection experiment performed in a gelatin sample. Successful insertion and deflection is demonstrated.

The needle compensation experiments shows a massive improvement in the needle retraction. At an insertion depth of 0mm the retraction was reduced to 0.5mm which is a reduction to 2.35% of the original retraction, at an insertion depth of 50mm the retraction was reduced to 2mm which is a reduction to 8.6% of the original retraction and at an insertion depth of 100mm the retraction was reduced to 2mm which is a reduction to 6.5% of the original retraction. Furthermore, there are no changes in compensation when switching between different insertion depths.

Experiment 1: Needle steering in cervix phantom: During the first experiment in the MR environment all three targets 5x5 mm targets were reached successfully at the first attempt from the same starting position as shown in figure 9.

Circumventing organs at risk (OARs) in prostate phantom: During this experiment the needle was unable to penetrate the phantom further than 30mm at this point the needle would start buckling.

During second attempt all 1 mm diameter targets were targeted using several different trajectories. Figure 10 shows a real time image and a high resolution image of the phantom.

To quantify the final distance between the needle tip and the target position figure 11 shows the segmented needle trajectories and the resulting error between the needle tip and target position. The average error is 1.2mm (n=10).

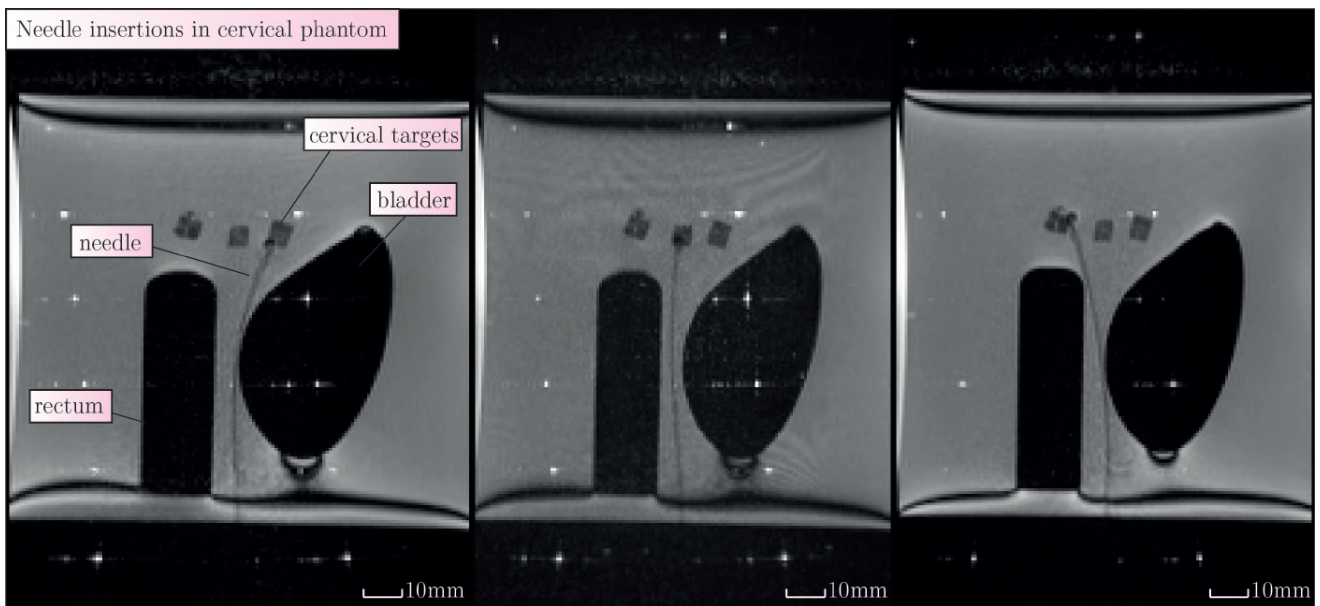


Fig. 9. Results of first experiment in the MR environment, all three images are the results of a single procedure. The left image shows the first target reached, the needle, the rectum and the bladder. The top right shows the second target reached and the bottom right image shows the final target reached.

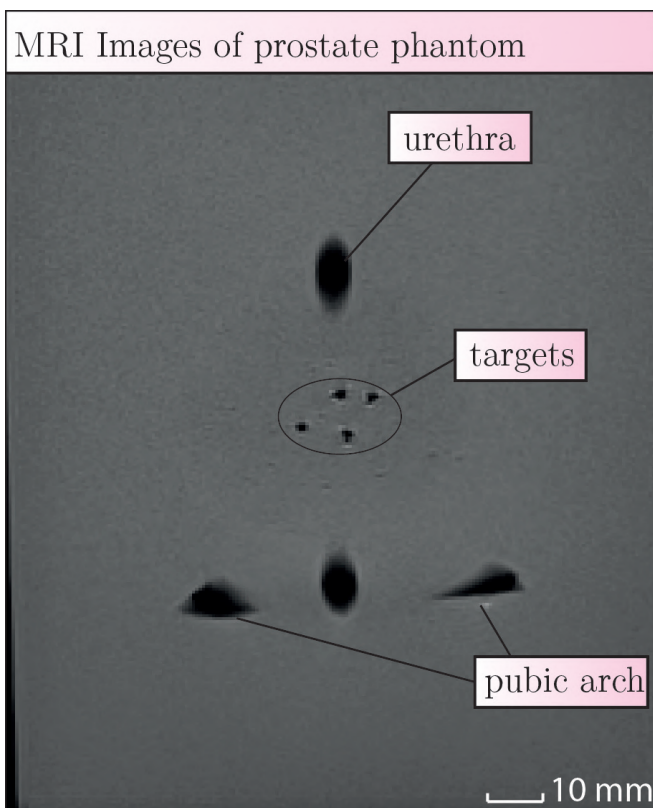


Fig. 10. A real time image with the needle inserted towards a target visualized of the prostate phantom on the left and a high resolution image of the prostate phantom visualized on the right.

VI. DISCUSSION

The goal of this work was to perform teleoperated needle steering in a MR environment, this was successfully performed

and demonstrated in several experiments. However, some limitations and possible improvement of the system are found. These will be highlighted in the next section.

A. MRI compatible needle steering

As mentioned in section II-B the MIRIAM system has limited movement possibilities in the vertical direction. The way the needle is actuated limits the current system of only actuating the needle in the horizontal plane. For clinical application steering in both the horizontal and vertical plane is desired. For this reason MIRIAM would require adaptations to increase its workspace.

With the current capabilities real-time MRI is still limited. In order to achieve high frame-rates the imaging resolution has to be relatively low, this is visible especially in figure 11. In addition to this low resolution the MIRIAM system introduces noise to the MRI when the motors are running. This could be (partially) solved by increasing the motor shielding. During the experiments an artifact occurs around the needle tip. This artifact is characteristic for needle tips in MRI under certain conditions [21].

B. Teleoperating MIRIAM with DaVinci Surgical system

There are also some limitations that relate to the teleoperation of the system. One of these limitations of the system is its speed, with the current movement speed much of the procedure is spent waiting for the MIRIAM system to catch up to the set-point. This is partly down to the piezo-electric motors and the rod designs, the piezo-electric motors that actuate the rods are placed on the outer diameter of a cylinder. Alignment of the motor on this cylinder highly influences performance of the motor. As the linear movement of the motor is transferred to a rotary motion there is a gear ratio applied to make sure

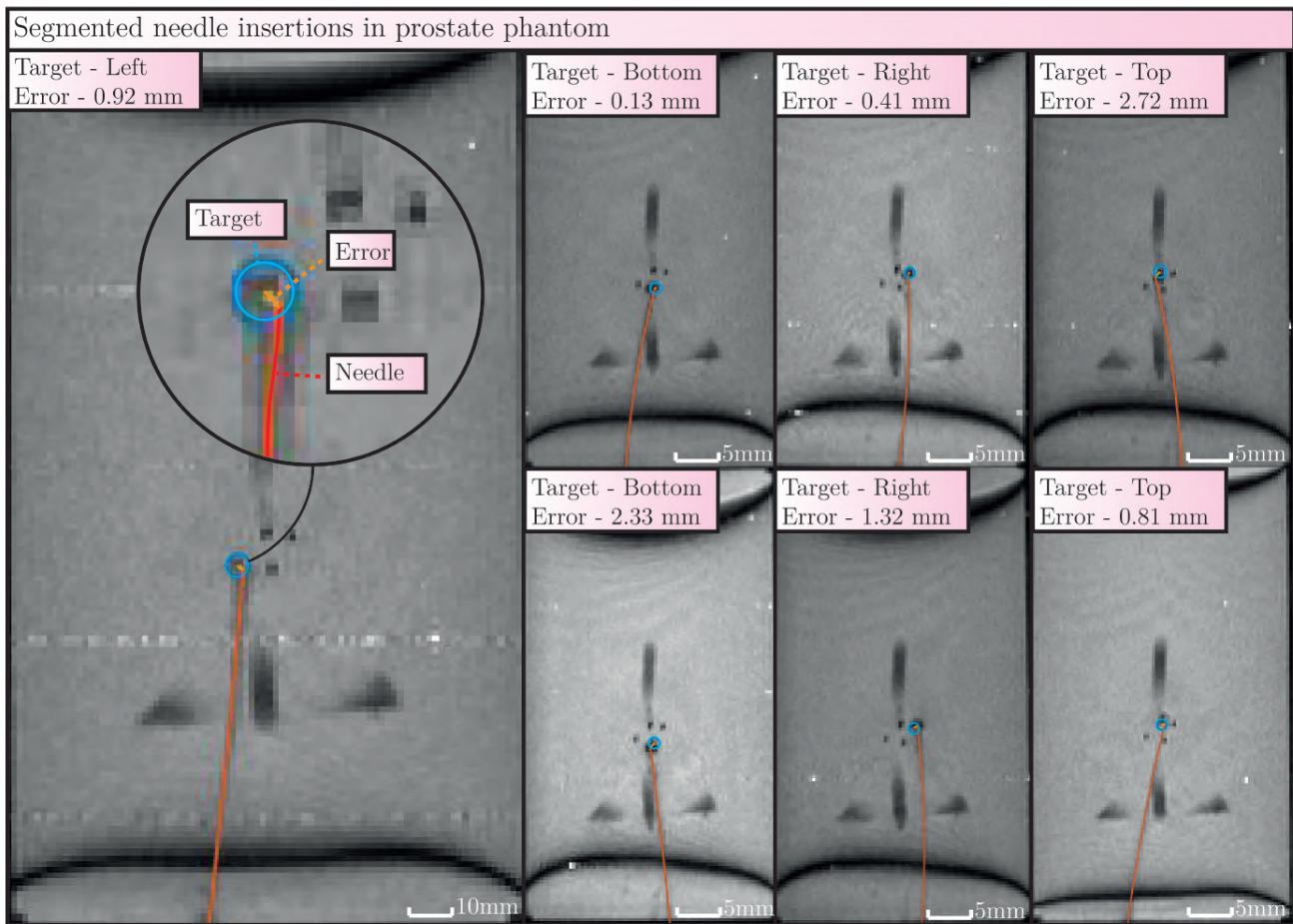


Fig. 11. Results of final experiment in the MR environment, the images show several possible trajectories to the targets. The needle is segmented this is visualised by the red line, the last millimeters are estimated by extending a polynomial fit to the needle. The target is selected and visualised by the blue circle. The error between the needle tip and the target is determined for each insertion and visualised by the orange line.

the motor has enough torque to move the rod. While this gear ratio enhances the torque it decreases the speed and results in relatively slow movement. The other contributing factor is the software limitation, since MIRIAM was designed for single set-point movement and not for continuous motion a trade-off between speed and accuracy has to be made. This is so deeply embedded in the original functionality of the MIRIAM system that the decision was made to implement a solution that solves the result but not the root of the problem. A solution for this would be recoding the software for MIRIAM to work with real time inputs.

While the current visualisation setup works it is not ideal as it gives the clinician limited control over the MRI settings. Ideally for future work a remote control setup could be implemented to give the clinician more control over the MRI scanning procedure [22].

C. Experiments

The experiments showed that needle steering can successfully be performed in gelatin phantoms. However, in phantoms with realistic tissue properties the system still has some limitations. The stiffness of the tissue combined with the

increasing friction forces at deeper insertions caused the needle to buckle at insertions deeper than 30mm. This issue could be solved by supporting the needle with an outer sheath that limits the amount of bending to prevent buckling. This sheath is quite a task to design without it impeding the insertion of the needle. Another solution would be to design a more rigid needle that is more resistant to buckling. The third experiment was performed to show the principal functionality of the needle that could in future be improved to prevent buckling in tissues that create higher resisting forces than gelatin. The final experiment was performed using the same anatomical structure but the material was much less stiff. This showed that the system can perform needle steering in a MR environment but that the needle and the support of the needle requires improvements for puncturing stiffer human tissue.

VII. CONCLUSIONS

This paper describes the possible application of robotic needle steering for prostate brachytherapy in a MR environment. An integrated system using the MIRIAM platform, a flexible needle and dVRK hardware is presented. This system demonstrates the ability to perform teleoperated needle steering in

a MR environment. Targets of 1mm diameter at 80-100mm depth are reached with an average error of 1.2mm (n=10). Real-time MR provides the ability to continuously monitor the needle position and to adjust the trajectory continuously during the procedure. The system is plug and play which allows it to be used in a MR room with very minimal adaptations. The experiments performed show that in gelatin samples and a single plane the system can robotically steer flexible needles using MRI guidance.

Future improvements to the MIRIAM and needle system could advance this application to clinical relevance. Higher movement speed of the system is desired to decrease procedure time. Furthermore, a balance should be found between image speed and resolution as the current resolution of the images is too low to accurately determine if the needle placement is correct. Finally improvements in stiffness or support of the needle will allow the system to function properly with stiffer phantoms and tissues.

ACKNOWLEDGMENT

The authors would like to thank Remco Liefers for the assistance in the execution of the experiments. This research has received funding from the Netherlands Organization for Scientific Research (Innovational Research Incentives Scheme VIDI: SAMURAI project 14855).

REFERENCES

- [1] Mathers *et al.*, "Global and regional causes of death," *British Medical Bulletin*, vol. 92, no. 1, pp. 7–32, Sep. 2009, ISSN: 0007-1420. DOI: 10.1093/bmb/ldp028.
- [2] Siegel *et al.*, "Cancer statistics, 2018," *CA: A Cancer Journal for Clinicians*, vol. 68, pp. 7–30, 1 Jan. 2018, ISSN: 00079235. DOI: 10.3322/caac.21442.
- [3] Galalae *et al.*, "Hypofractionated conformal HDR brachytherapy in hormone naïve men with localized prostate cancer," *Strahlentherapie und Onkologie*, vol. 182, pp. 135–141, 3 Mar. 2006, ISSN: 0179-7158. DOI: 10.1007/s00066-006-1448-5.
- [4] Koukourakis *et al.*, "Brachytherapy for prostate cancer: A systematic review," *Advances in Urology*, vol. 2009, pp. 1–11, 2009, ISSN: 1687-6369. DOI: 10.1155/2009/327945.
- [5] Kamrava *et al.*, "Brachytherapy in the treatment of cervical cancer: A review," *International Journal of Women's Health*, p. 555, May 2014, ISSN: 1179-1411. DOI: 10.2147/IJWH.S46247.
- [6] Brass *et al.*, "Percutaneous techniques versus surgical techniques for tracheostomy," *Cochrane Database of Systematic Reviews*, Jul. 2016, ISSN: 14651858. DOI: 10.1002/14651858.CD008045.pub2.
- [7] Fischer-Valuck *et al.*, "A brief review of low-dose rate (LDR) and high-dose rate (HDR) brachytherapy boost for high-risk prostate," *Frontiers in Oncology*, vol. 9, Dec. 2019, ISSN: 2234-943X. DOI: 10.3389/fonc.2019.01378.
- [8] Nayak *et al.*, "Real-time magnetic resonance imaging," *Journal of Magnetic Resonance Imaging*, vol. 55, pp. 81–99, 1 Jan. 2022, ISSN: 1053-1807. DOI: 10.1002/jmri.27411.
- [9] Siebert *et al.*, "Imaging of implant needles for real-time HDR-brachytherapy prostate treatment using bi-plane ultrasound transducers," *Medical Physics*, vol. 36, pp. 3406–3412, 8 Jul. 2009, ISSN: 00942405. DOI: 10.1118/1.3157107.
- [10] Sadjadi *et al.*, "Needle deflection estimation: Prostate brachytherapy phantom experiments," *International Journal of Computer Assisted Radiology and Surgery*, vol. 9, pp. 921–929, 6 Nov. 2014, ISSN: 1861-6410. DOI: 10.1007/s11548-014-0985-0.
- [11] Veen *et al.*, "Macroscopic and microscopic observations of needle insertion into gels," *Proceedings of the Institution of Mechanical Engineers, Part H: Journal of Engineering in Medicine*, vol. 226, pp. 441–449, 6 Jun. 2012, ISSN: 0954-4119. DOI: 10.1177/0954411912443207.
- [12] Moreira *et al.*, "Evaluation of robot-assisted MRI-guided prostate biopsy: Needle path analysis during clinical trials," *Physics in Medicine Biology*, vol. 63, 20NT02, 20 Oct. 2018, ISSN: 1361-6560. DOI: 10.1088/1361-6560/aae214.
- [13] Moreira *et al.*, "A preliminary evaluation of a flexible needle steering algorithm using magnetic resonance images as feedback," *IEEE*, Aug. 2014, pp. 314–319, ISBN: 978-1-4799-3128-6. DOI: 10.1109/BIOROB.2014.6913795.
- [14] Misra *et al.*, "Mechanics of flexible needles robotically steered through soft tissue," *The International Journal of Robotics Research*, vol. 29, pp. 1640–1660, 13 Nov. 2010, ISSN: 0278-3649. DOI: 10.1177/0278364910369714.
- [15] Abayazid *et al.*, "Experimental evaluation of co-manipulated ultrasound-guided flexible needle steering," *The International Journal of Medical Robotics and Computer Assisted Surgery*, vol. 12, pp. 219–230, 2 Jun. 2016, ISSN: 14785951. DOI: 10.1002/rcs.1680.
- [16] Moreira *et al.*, "Tele-operated MRI-guided needle insertion for prostate interventions," *Journal of Medical Robotics Research*, vol. 04, no. 01, p. 1842003, 2019. DOI: 10.1142/S2424905X18420035.
- [17] Moreira *et al.*, "The Miriam robot: A novel robotic system for MRI-guided needle insertion in the prostate," *Journal of Medical Robotics Research*, vol. 02, p. 1750006, 04 Dec. 2017, ISSN: 2424-905X. DOI: 10.1142/S2424905X17500064.
- [18] Vries *et al.*, "Axially rigid steerable needle with compliant active tip control," *PLOS ONE*, vol. 16, e0261089, 12 Dec. 2021, ISSN: 1932-6203. DOI: 10.1371/journal.pone.0261089.
- [19] Wang *et al.*, "MRI compatibility evaluation of a piezoelectric actuator system for a neural interventional robot," *IEEE*, Sep. 2009, pp. 6072–6075. DOI: 10.1109/IEMBS.2009.5334206.
- [20] D'Etorre *et al.*, "Accelerating surgical robotics research: A review of 10 years with the da Vinci research

- kit,” *IEEE Robotics Automation Magazine*, vol. 28, pp. 56–78, 4 Dec. 2021, ISSN: 1070-9932. DOI: 10.1109/MRA.2021.3101646.
- [21] Liu *et al.*, “Biopsy needle tip artifact in mr-guided neurosurgery,” *Journal of Magnetic Resonance Imaging*, vol. 13, no. 1, pp. 16–22, 2001. DOI: [https://doi.org/10.1002/1522-2586\(200101\)13:1<16::AID-JMRI1003>3.0.CO;2-B](https://doi.org/10.1002/1522-2586(200101)13:1<16::AID-JMRI1003>3.0.CO;2-B).
- [22] Lohan *et al.*, “Mri scanning by remote control: Experience in pediatric cardiovascular disease,” *Journal of Cardiovascular Magnetic Resonance*, vol. 12, P30, S1 Jan. 2010, ISSN: 1532-429X. DOI: 10.1186/1532-429X-12-S1-P30.

Chapter 3

Discussions

This thesis describes the design and control of a robotic needle steering device for MRI guided brachytherapy. For this project three pre-developed systems were adapted and integrated. The MIRIAM robotic system was resurrected, updated and adapted for a different application. The axial stiff steerable needle with compliant active tip control provided by the 3ME group at the Technical University Delft was integrated with the MIRIAM robotic system and robotically actuated for the first time. Finally the daVinci Research kit at the SRL was integrated with the MIRIAM robot showing its potential to be applied to many medical robotics applications. Many aspect of this project show great potential for future work with several of the systems used in this project.

Conclusions

The goal of this work was to develop a MRI-guided needle insertion system for BT. The system integrates an active needle, a MRI-compatible needle insertion robot, and a teleoperating platform. This goal was successfully achieved and was demonstrated through several experiments.

Appendices

Appendix A

Production of a gelatin prostate phantom

This appendix describes how a gelatin prostate phantom was produced. The phantom was used for MRI guided Brachytherapy using flexible needles. A step wise approach was followed for the production of a prostate gelatin phantom, first the components will be explained and visualized after which the method is explained.

Components

The following components are used to create the phantom.

- Plexiglas container
- Prostate mould
- Pubic arch
- urethra — 5mm flexible tube
- rectum
- carbon target rods 1mm diameter

Several of these components are visualised in figure 1

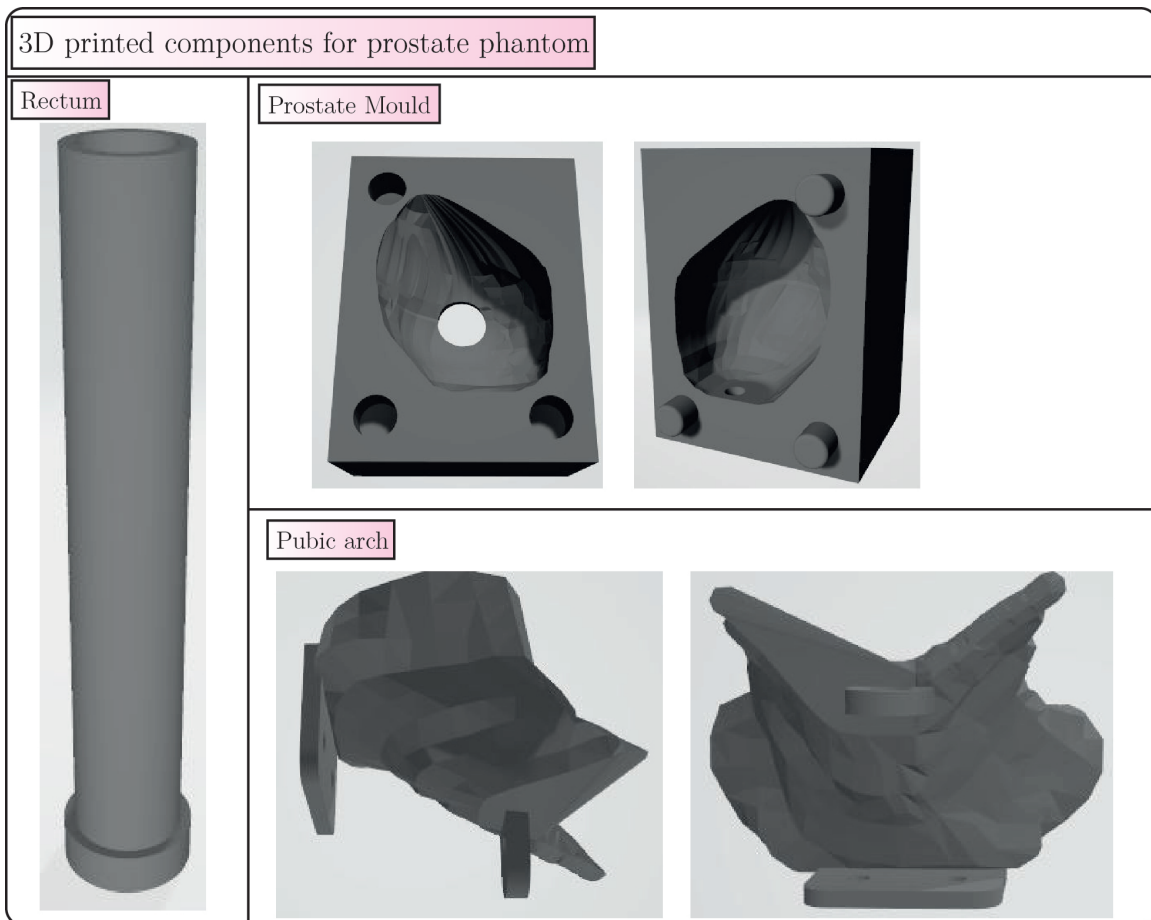


Figure 1: Shows the 3D printed components used for the production of a gelatin prostate phantom

Production method

The phantom was produced using the following steps:

1. Laser cut a container to house the gelatin phantom, the plexiglas housing is glued using chloroform. Additional waterproofing is provided by glueing the edges with hot glue.
2. Boil water and mix with gelatin powder at a 100g of gelatin per liter water, add Sudan Orange G until desired amount of colour is achieved.
3. Glue plastic tube with 5mm diameter into mould to waterproof.
4. Mount mould together with thin layer of rubber in between for waterproofing. If the 3d printed mould is porous it can be submerged in water, removed and frozen to freeze water inside.
5. Pour gelatin mixture into mould and place in fridge.
6. Place 3d printed rectum in container and waterproof with hot glue.
7. Mount pubic arch to top of container
8. After 24 hours remove prostate from mould and suspend from top of container using urethra as guide.
9. Boil water and mix with gelatin powder at a 100g of gelatin per liter water, let cool down significantly to prevent melting the prostate.
10. Pour gelatin mixture into container and set in fridge.
11. After 24 hours, remove top of container keeping pubic arch and urethra in place, remove prostate and remove front of container.

These steps were followed to create the prostate phantom as presented in figure 2

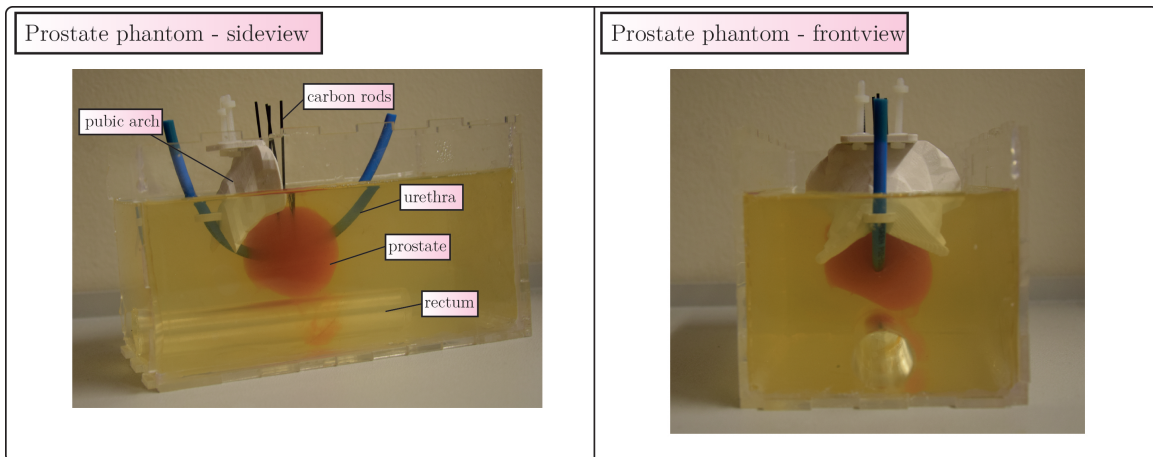
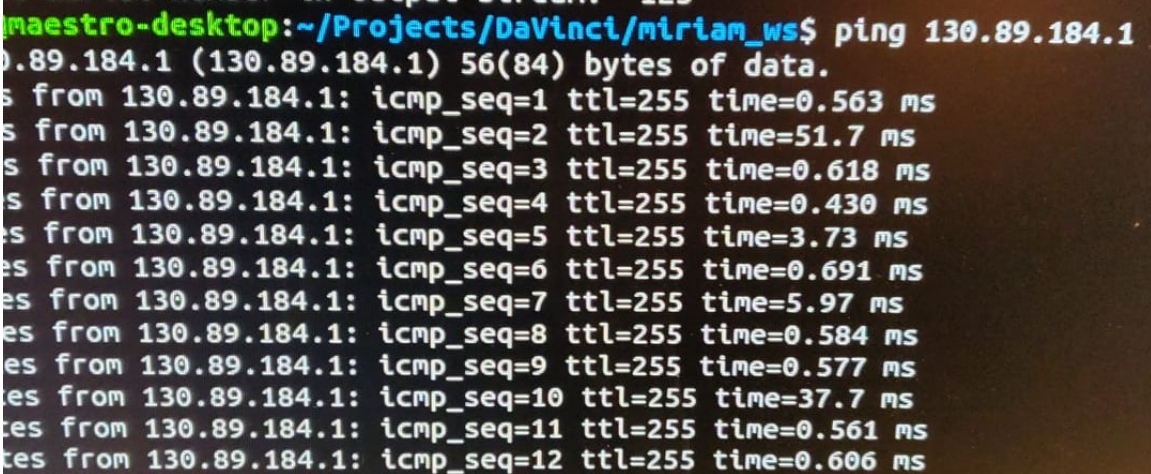


Figure 2: Gelatin prostate phantom created using method explained in appendix A

Appendix B

Remote system latency test

As presented in the paper a latency test between a system placed in the Horst building at the University of Twente and a system in the Techmed Centre at the University of Twente was performed. The results of this test are shown in figure 3. The average latency of this test resulted in 8.5 ms with a min latency of 0.43 ms and a maximum latency of 51.7 ms.



```
maestro-desktop:~/Projects/DaVinci/miriam_ws$ ping 130.89.184.1
130.89.184.1 (130.89.184.1) 56(84) bytes of data:
64 bytes from 130.89.184.1: icmp_seq=1 ttl=255 time=0.563 ms
64 bytes from 130.89.184.1: icmp_seq=2 ttl=255 time=51.7 ms
64 bytes from 130.89.184.1: icmp_seq=3 ttl=255 time=0.618 ms
64 bytes from 130.89.184.1: icmp_seq=4 ttl=255 time=0.430 ms
64 bytes from 130.89.184.1: icmp_seq=5 ttl=255 time=3.73 ms
64 bytes from 130.89.184.1: icmp_seq=6 ttl=255 time=0.691 ms
64 bytes from 130.89.184.1: icmp_seq=7 ttl=255 time=5.97 ms
64 bytes from 130.89.184.1: icmp_seq=8 ttl=255 time=0.584 ms
64 bytes from 130.89.184.1: icmp_seq=9 ttl=255 time=0.577 ms
64 bytes from 130.89.184.1: icmp_seq=10 ttl=255 time=37.7 ms
64 bytes from 130.89.184.1: icmp_seq=11 ttl=255 time=0.561 ms
64 bytes from 130.89.184.1: icmp_seq=12 ttl=255 time=0.606 ms
```

Figure 3: Latency test between MIRIAM system placed in MRI room and dVRK system placed in Surgical Robotics Lab